ISSN 1063-7850, Technical Physics Letters, 2021, Vol. 47, No. 8, pp. 765–768. © Pleiades Publishing, Ltd., 2021.
Russian Text © The Author(s), 2021, published in Pis'ma v Zhurnal Tekhnicheskoi Fiziki, 2021, Vol. 47, No. 15, pp. 27–30.

Simulating the Conditions for Cooling Bismuth Germanate Bi_2GeO_5

T. V. Bermeshev[a]*, V. P. Zhereb[a,b], I. Yu. Gubanov[a], A. B. Nabiulin[c], V. P. Chentsov[d], V. V. Ryabov[d], A. S. Yasinskii[a,e], N. V. Merdak[a], O. V. Yushkova[a], M. P. Bundin[a], V. M. Bespalov[a], E. V. Mazurova[f], D. S. Voroshilov[a], and E. Yu. Podshibyakina[a]

[a] *Siberian Federal University, Krasnoyarsk, 660041 Russia*
[b] *Siberian State University of Science and Technology, Krasnoyarsk, 660037 Russia*
[c] *OOO Krasnoyarsk Boiler Plant, Krasnoyarsk, 660013 Russia*
[d] *Institute of Metallurgy, Ural Branch, Russian Academy of Sciences, Yekaterinburg, 620016 Russia*
[e] *Institute for Process Metallurgy and Metal Recycling, RWTH Aachen University, Aachen, 52056 Germany*
[f] *Institute of Chemistry and Chemical Technology, Krasnoyarsk Scientific Center, Siberian Branch, Russian Academy of Sciences, Krasnoyarsk, 660036 Russia*
**e-mail: irbis_btv@mail.ru*

Received April 5, 2021; revised April 30, 2021; accepted April 30, 2021

Abstract—The possibility of modeling the processes of cooling of the metastable Bi_2GeO_5 compound in the ProCAST software package is demonstrated. Despite a number of assumptions that are made in the modeling, the calculated data are shown to be in good agreement with the real melt cooling rates and can be used in the development of modeling in the Bi_2O_3–GeO_2 system to obtain metastable materials with a desired set of properties and a microstructure.

Keywords: bismuth germanate, metastable compound, modeling, cooling time, crystallization.
DOI: 10.1134/S1063785021080046

Metastable bismuth germanate Bi_2GeO_5 with an Aurivillius layered crystal structure, which is formed during crystallization of a supercooled melt, is a ferroelectric with the high Curie temperature, high oxygen ionic conductivity, and unique catalytic properties. It is of great interest for hydrogen energetics and ecology due to its photocatalytic properties in the optical radiation range—in particular, for deactivation of toxic organic compounds and nitrogen oxides (NOs) and as a catalyst for the oxidative dimerization of methane. In addition, this compound is used in the synthesis of advanced glass-ceramic materials.

The Bi_2O_3–GeO_2 system is represented by a stable state diagram and two metastable ones. According to the results obtained in [1–4], the region of the liquid state in the phase diagram of the Bi_2O_3–GeO_2 system was divided into three temperature zones *A*, *B*, and *C*, the melt cooling from which (from cooling start temperatures $t_{st.cool.}$) affects differently the state of the synthesized crystalline phases. The existence of the temperature zones and the impact of the melt cooling conditions on the composition of the formed crystalline phases were experimentally confirmed in [5, 6].

The methods for obtaining Bi_2GeO_5 (hydrothermal synthesis, deposition, quenching and annealing, solid-state synthesis, sol–gel, etc.) have certain advantages and benefits, but still, for the most part, are rather labor- and time-consuming and require significant costs, additional equipment, and reaction components. In [6], we managed to reliably demonstrate that the method for synthesizing these layered compounds from melt is not only possible, but also the simplest and most convenient under conventional heat treatment of the melt. To implement this method, only the initial components Bi_2O_3 and GeO_2, a crucible, and a furnace are needed.

Taking into account that the synthesis of metastable bismuth germanate Bi_2GeO_5 from melt is one of the fastest and simplest ways to obtain this promising material, the question arises of whether it is possible to model the heating and cooling processes for obtaining this compound with a desired set of properties and a microstructure.

This Letter systematizes the available thermal characteristics, attempts to model the conditions for cooling the metastable Bi_2GeO_5 compound using the ProCAST software package, and evaluates the results obtained by comparing them with the experimental data.

Table 1. Thermal characteristics of Bi_2GeO_5 as functions of temperature

t, °C	C_p, J/(mol K)	t, °C	ρ, g/cm^3
82	174 [8]	20	7.4817
127	179 [8]	1297	7.66 [7]
227.1	188 [8]	t, °C	λ, W/(m K)
327	195 [8]	299	1.02
427.1	201 [8]	400	0.95
527	206 [8]	500	1.07
627.1	211 [8]	600	1.35
727	217 [8]	700	1.89
827	**224**	*1067*	*0.20* [9]
927	**230**		
1027	**237**		
1127	**243**		
1227	**249**		

The density of the material was measured at room temperature with a Vibra HT automatic analytical balance by hydrostatic weighing and then taken as a constant up to the solidus temperature. The melt density at a temperature of 1297°C was borrowed from [7] and also taken as a constant up to the liquidus temperature.

The liquidus and solidus temperatures for the calculation were taken in accordance with the metastable equilibrium diagrams. Depending on the cooling start temperature, they were 837 and 820°C for zone *C* and 879°C for zone *B*.

With regard to the preservation of the metastable state of the melt after its heat treatment [6], to calculate the melt cooling from zone *A*, the liquidus and solidus values were taken for the metastable phase diagram obtained by cooling from zone *B*, rather than for the stable one.

Similar assumptions were made for the thermal conductivity coefficient.

The heat capacity values at a temperature in the range of 82–727°C were taken from [8] and continued to a temperature of 1227°C by the mathematical prediction method (the calculation using Eq. (1), which describes a linear approximation, where x is the heating temperature)

$$y = 0.0629x + 172.1. \quad (1)$$

The thermal diffusivity was measured on a Netzsch LFA 457 MicroFlash setup. Thermal conductivity coefficient λ was calculated using to the formula

$$\lambda = \alpha C_p \rho, \quad (2)$$

where α is the thermal diffusivity, C_p is the heat capacity of the material, and ρ is the density of the material.

The density was calculated as

$$\rho = m/v, \quad (3)$$

where m is the mass of the sample and v is its volume. The porosity of the material was ignored.

To the best of our knowledge, the thermal conductivity of the melt of the metastable Bi_2GeO_5 (1 : 1 Bi_2O_3–GeO_2) compound has not been investigated, and we failed to find such data in the literature. Therefore, the thermal conductivity of the closest stable compound $Bi_4Ge_3O_{12}$ (2 : 3 Bi_2O_3–GeO_2) studied in [9] was taken as a thermal conductivity of the melt for our primary calculation. In Table 1, this value is put in italics.

The material of the crucible was pure platinum. The geometry of the product corresponds to product no. 100-10 (*GOST* (State Standard) 6563–75). The weight of the sample for melting was 10 g. The crystallized melt thickness was 1.97–2.4 mm. The thermal characteristics of the crucible material (pure platinum) were taken from [10].

Modeling was carried out using the ProCAST professional software package. The calculation repeated the nine cooling regimes reported in [6] (Fig. 1). The only difference from study [6] was that the furnace cooling was performed at a controlled rate (4°C/min) to compare the calculated and real crystallization rates in the maximally equilibrium conditions. The parameters for modeling the thermal problem were an ambient temperature of 20°C, a water temperature of 15°C, and a liquidus temperature of platinum of 1768°C. The heat transfer coefficient was 10000 W/(m^2 K) for melt–crucible, 5000 W/(m^2 K) for crucible–water, and 300 W/(m^2 K) for crucible–firebrick.

The thermal characteristics (heat capacity C_p, density ρ, and thermal conductivity λ) of the Bi_2GeO_5 compound as functions of temperature are given in Table 1. The values obtained using the mathematical prediction are highlighted in bold, and the thermal conductivity of the melt taken from the closest stable compound $B_4Ge_3O_{12}$ (2 : 3 Bi_2O_3–GeO_2) [9] is italicized.

According to the modeling results, Fig. 2a shows an example of the cooling time distribution over the cross section of the material in a crucible during water quenching of the melt in a crucible from zone *C* (regime *3* in Fig. 1a). A similar distribution upon cooling the melt from liquidus to solidus is shown in Fig. 2b.

The time dependences of temperature during cooling of the melt to room temperature in the regimes illustrated in Fig. 1 are given in Table 2 and shown in Fig. 3 as an example of quenching. The calculation shows that, during water quenching (Fig. 3), the rate of melt cooling in the central part of a crucible and at a distance of 0.5R (R is the radius of the model simulating the volume of the cooled melt from the center of

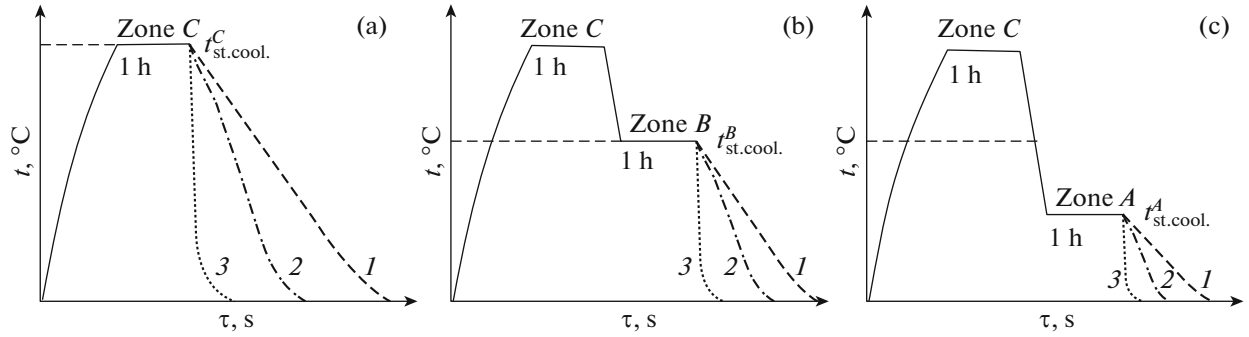

Fig. 1. Scheme of regimes of heat treatment of the melt upon cooling from cooling start temperatures $t_{st.cool.}$ from temperature zones (a) *C*, (b) *B*, and (c) *A*. (*1*) Furnace cooling, (*2*) cooling in air, and (*3*) water cooling of a crucible.

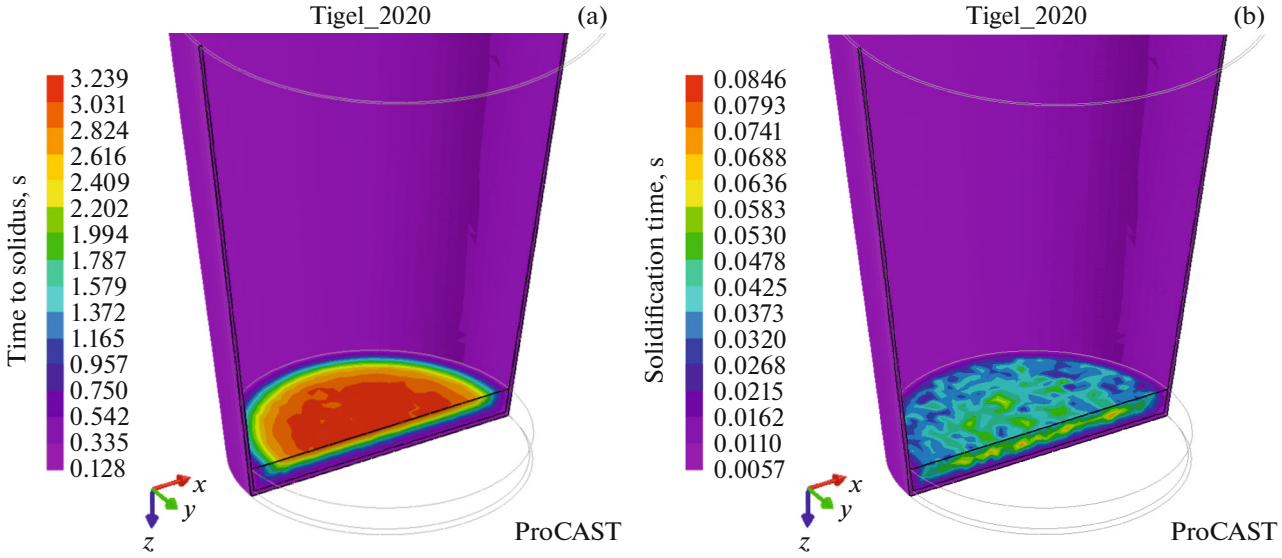

Fig. 2. Cooling time distribution over the cross section of the sample (melt) in a crucible during quenching from zone *C* ($t_{st.cool.}$ = 1160°C). (a) Cooling to complete crystallization and (b) cooling from the liquidus to solidus temperature of the alloy.

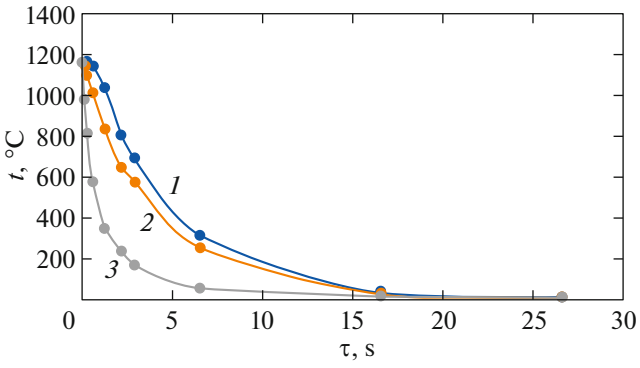

Fig. 3. Time dependence of temperature during quenching from zone *C* ($t_{st.cool.}$ = 1160°C) (*1*) in the central part of a crucible and at distances of (*2*) 0.5*R* and (*3*) 0.9*R*.

a crucible to its inner wall) is almost the same and differs only at the periphery, i.e., at the crucible walls and the bottom, where the heat removal is fastest. This fact will also be affected by the amount of melt and the crucible geometry. Upon cooling in air from the cooling start temperature to complete cooling, the rate of melt cooling over the cross section in a crucible will differs less than upon water quenching. Under furnace cooling, the material will have a minimum temperature gradient between layers. It can be seen in Table 2 that the calculated values for both the crystallization time and complete cooling are in good agreement with each other and have no rough and clearly noticeable drops.

Comparison of the calculated cooling time with the real values (Table 2) confirms our conclusions once

Table 2. Times of crystallization and complete cooling of the 1 : 1 Bi_2O_3–GeO_2 melt upon cooling from different start temperatures in different regimes obtained using the mathematical modeling in the ProCAST software package (comparison of the calculated and real melt crystallization times)

$t_{st.cool.}$, °C	Regime for cooling a crucible with melt	Calculated crystallization time, s (rounded off to the nearest integer)	Real crystallization time, s	Calculated complete cooling	
				Temperature, °C (crucible center control, rounded off to the nearest integer)	Time, s (rounded off to the nearest integer)
1160	Water quenching	3	5–8	36	17
	Cooling in air	17	24	36	392
	Furnace cooling	5115	5100	360	12011
1102	Water quenching	3		8	16
	Cooling in air	13		38	356
	Furnace cooling	3368		360	11 141
1037	Water quenching	2		56	14
	Cooling in air	10		57	236
	Furnace cooling	2394		360	10 171

again and shows good agreement between the theoretical modeling data and the proven results.

Thus, we demonstrated the possibility of modeling the processes of cooling of the metastable Bi_2GeO_5 compound with an Aurivillius crystal structure using the ProCAST software package. The modeling results showed good agreement between the calculated and real melt cooling rates. This method of calculation in the ProCAST software package is applicable for modeling the processes of heating and cooling of the metastable Bi_2O_3–GeO_2 compounds in order to obtain them with a desired set of properties and a microstructure, which is of great importance for fundamental research and application.

ACKNOWLEDGMENTS

The equipment of the Krasnoyarsk Regional Center for Collective Use, Krasnoyarsk Scientific Center of the Siberian Branch of the Russian Academy of Sciences, was used.

FUNDING

This study was carried out within the framework of a state order from the Ministry of Science and Higher Education of the Russian Federation, theme code FSRZ-2020-0013.

CONFLICT OF INTEREST

The authors declare that they have no conflicts of interest.

REFERENCES

1. I. V. Tananaev, V. M. Skorikov, Yu. F. Kargin, and V. P. Zhereb, Izv. Akad. Nauk SSSR, Neorg. Mater. **14**, 2024 (1978).
2. V. P. Zhereb, Yu. F. Kargin, and B. M. Skorikov, Izv. Akad. Nauk SSSR, Neorg. Mater. **14**, 2029 (1978).
3. V. P. Zhereb and V. M. Skorikov, Inorg. Mater. **39**, S121 (2003). https://doi.org/10.1023/B:INMA.0000008890.41755.90
4. V. P. Zhereb, *Metastable States in Oxide Bismuth-Containing Systems* (MAKS Press, Moscow, 2003) [in Russian].
5. G. Corsmit, M. A. van Driel, R. J. Elsenaar, W. van de Guchte, A. M. Hoogenboom, and J. C. Sens, J. Cryst. Growth **75**, 551 (1986).
6. V. P. Zhereb, T. V. Bermeshev, Yu. F. Kargin, E. V. Mazurova, and V. M. Denisov, Inorg. Mater. **55**, 737 (2019). https://doi.org/10.1134/S0020168519060165
7. V. P. Zhereb, Extended Abstract of Cand. Sci. Dissertation (Kurnakov Inst. Gen. Inorg. Chem., Moscow, 1980).
8. L. T. Denisova, N. V. Belousova, N. A. Galiakhmetova, V. M. Denisov, and V. P. Zhereb, Phys. Solid State **59**, 1683 (2017). https://doi.org/10.1134/S106378341708008X
9. V. D. Golyshev, M. A. Gonik, and V. B. Tsvetovsky, High Temp. High Press. **35–36**, 139 (2003–2004). https://doi.org/10.1068/htjr106
10. V. E. Zinov'ev, *Thermophysical Properties of Metals at High Temperatures, The Handbook* (Metallurgiya, Moscow, 1989) [in Russian].

Translated by E. Bondareva